VO_2(B) nanorods: solvothermal preparation, electrical properties, and conversion to rutile VO_2 and V_2O_3†

Serena A. Corr,*[a] Madeleine Grossman,[a] Yifeng Shi,[b] Kevin R. Heier,[c] Galen D. Stucky[ab] and Ram Seshadri[ab]

Received 19th January 2009, Accepted 4th March 2009
First published as an Advance Article on the web 31st March 2009
DOI: 10.1039/b900982e

The solvothermal reduction of V_2O_5 by formaldehyde or isopropanol yields nanorods of the metastable, monoclinic VO_2(B) phase. The structural transition in VO_2(B), which occurs near room temperature, has been monitored using electrical resistivity measurements, performed both on pressed pellets of the nanorods as well as on nanorods dispersed on patterned contacts. A sudden, 10^5 increase in the electrical resistivity upon cooling below 290 K is seen in measurements on VO_2(B) samples. Such a transition in the electrical resistivity has not previously been reported in this material. The transition is reminiscent of the metal-to-insulator transition observed in the case of pressed pellets of polycrystalline rutile VO_2 upon cooling below 340 K. The metastable VO_2(B) nanorods are converted to rutile VO_2 by heating in argon, and to corundum V_2O_3 by reducing in $5\%H_2:95\%N_2$. In both transformations, the structural integrity of the nanorods is compromised, with large, dense, rutile VO_2 crystallites and less well-defined nanorods of V_2O_3 being formed.

Introduction

Vanadium oxide materials have received considerable attention as a consequence of the rich number of structural and compositional variants, along with their use in a number of applications.[1] In addition, several vanadium oxides display interesting physical properties including metal–insulator transitions. The rutile modification of VO_2 in particular, famously undergoes an insulator-to-metal transition at 340 K with a many-thousand-fold increase in its conductivity.[2] Associated with this transition is a structural distortion from a monoclinic phase to the high-temperature tetragonal structure.[3,4] The transition has been attributed to pairing of vanadium ions in the low-temperature monoclinic phase; V^{4+}–V^{4+} ions dimerizing along the *c*-axis leads to a shift of the π^* band away from the Fermi level and removal of the $d_{||}$ band degeneracy.[5] Detailed driving forces for the transition and the microscopic mechanism continue to attract attention.[6,7]

A metastable polymorph of VO_2 [referred to as VO_2(B)] is known to form upon soft-chemical synthesis.[8] This compound undergoes a structural transition near room temperature that is accompanied by an anomaly in the magnetic susceptibility. Based on X-ray powder diffraction studies, Oka *et al.*[9] have established that the structural transition in this compound arises as a result of a V^{4+}–V^{4+} dimerization, although the dimerization pattern is distinct from that observed in rutile VO_2. The structures, as determined by Oka *et al.*,[9] of the high (300 K) and low (50 K) temperature forms of VO_2(B) are displayed in Fig. 1. There is no change in the monoclinic space group across the phase transition. Curiously, and in striking contrast to the rutile modification, the electrical properties of VO_2(B) have so far not been reported across the phase transition temperature.

Important considerations for soft-chemical preparation of vanadium oxides—especially in nanostructured modifications—include the choice and concentration of vanadium precursor, reducing agent, surfactant, and the reaction temperature. For example, we have previously found that careful variation of reduction times and temperatures of amine-templated VO_x nanoscrolls selectively leads to rutile VO_2 or corundum V_2O_3

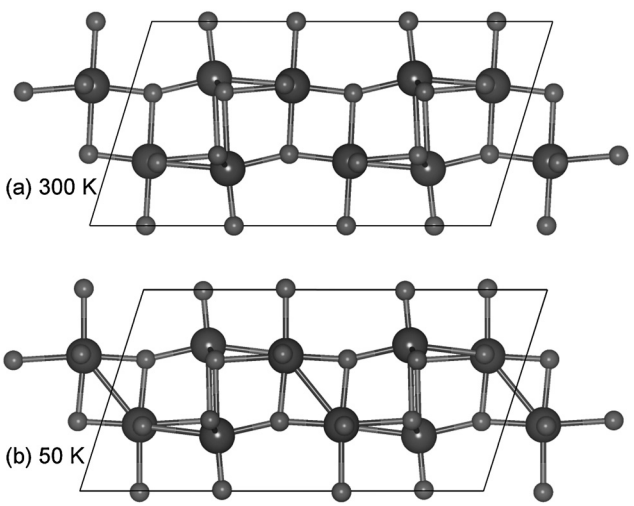

Fig. 1 Structure of the metastable, monoclinic VO_2(B) polymorph at (a) 300 K and (b) 50 K, as reported by Oka *et al.*[9] The dimerization of the V^{4+}–V^{4+} ions is apparent in the case of the low-temperature structure. Larger spheres are V atoms, while smaller are O atoms.

[a]*Materials Department and Materials Research Laboratory University of California, Santa Barbara, CA, 93106, USA. E-mail: serena@mrl.ucsb.edu; Fax: +805 893 8797*
[b]*Department of Chemistry and Biochemistry University of California, Santa Barbara, CA, 93106, USA*
[c]*Air Products and Chemicals Inc., Allentown, PA, 18195, USA*
† This paper is part of a *Journal of Materials Chemistry* issue in celebration of the 75th birthday of C. N. R. Rao.

nanostructures.[10] There are many reported routes to the monoclinic VO_2(B) phase. This metastable material is a useful precursor for the preparation of other vanadium oxides. For example, Pavasupree *et al.* have shown that treatment of a vanadium alkoxide/laurylamine hydrochloride mixture with acetylacetone afforded VO_2(B) nanorods, which, after calcination, gave orthorhombic V_2O_5 microrods.[11] In a study of the reduction effects of organic molecules on vanadium pentoxide, Li and coworkers found that VO_2(B) is formed when oxalic acid is used, while a partially reduced orthorhombic $H_2V_3O_8$ phase is found when ethanol is employed.[12] Nanobelts of the VO_2(B) phase are noted at lower oxalic acid concentrations, with larger three-dimensional structures formed at higher concentrations. Other routes to VO_2(B) include the hydrothermal treatment of ammonium metavanadate in the presence of formic acid,[13,14] vapor transport methods,[15] the ethylene glycol reduction of V_2O_5,[16,17] and the reaction between V_2O_5 and aniline or benzylamine.[18]

While rutile VO_2 finds potential applications in optical switching devices or in field-effect transitors, the metastable VO_2(B) phase has been investigated as a cathode material for rechargeable lithium batteries. Chen *et al.* have reported the treatment of V_2O_5 with CTAB, which acts as both a template and a reducing agent, affording metastable VO_2(B) nanowires which maintain 80% of their initial specific capacity.[19] Similar electrochemical behavior has been reported by Zhou *et al.*, who employed $VOSO_4 \cdot xH_2O$ as the vanadium source and polyethylene glycol as the reducing agent for the preparation of VO_2(B) nanorods.[20] Conversion of the metastable VO_2(B) phase to the more stable rutile form of VO_2 may be realized by heating under inert conditions. This transformation has been previously studied using electron diffraction and electron microscopy methods by Leroux *et al.*,[21] by heating up to 450 °C under low-pressure conditions. Transformation of metastable VO_2(B) nanorods, prepared by the reducion of ammonium metavanadate by formic acid, to rutile VO_2 has been previously reported by Kam *et al.*, following heating at 700 °C in N_2.[14]

Here we report the preparation in gram quantities of VO_2(B) nanorods by solvothermal reduction of V_2O_5 in neat 30% formaldehyde solution or in isopropanol. We report, for the first time, electrical property measurements on this interesting material and determine that the structural transition near room temperature is accompanied by a hysteretic change in the electrical resistivity, not dissimilar to what is seen in polycrystalline pellets of rutile VO_2. We also demonstrate the conversion of the metastable VO_2(B) nanorods to rutile VO_2 through heating in an inert atmosphere, and to corundum V_2O_3 through heating under a reducing atmosphere. Neither of these conversions is pseudomorphic and the original rod-like architecture is lost.

Experimental

Vanadium(V) oxide (1.81 g; 0.01 mol) was dispersed in formaldehyde (37% solution, 30 mL) or isopropanol (30 mL) by stirring for 2 h. The resulting yellow suspension was placed in a Paar bomb and hydrothermally treated for 2 days at 180 °C. After cooling to room temperature, the resulting blue-black powder was washed with water, ethanol and diethyl ether and dried overnight at 70 °C in a vacuum oven. Conversion to the rutile VO_2 phase was achieved by heating the metastable sample in argon at 700 °C for 1 h. This conversion was also monitored using *in situ* thermodiffractometry techniques. The room-temperature metallic V_2O_3 phase was obtained after reduction in $5\%H_2 : 95\%N_2$ at 600 °C for 3 h. All products were characterised by X-ray diffraction (XRD), scanning electron microscopy (SEM), transmission electron microscopy (TEM) and electrical property measurements. XRD patterns were obtained using a Philips XPert Pro X-ray diffractometer with Cu Kα radiation (1.5418 Å) at a 45 kV accelerating voltage and 40 mA. Powder patterns were analyzed using the Rietveld method as embodied in the Rietveld code.[22] *In situ* thermodiffractometry was done on a BrukerD8 Advance diffractometer fitted with an Anton Paar platinum high-temperature stage. Samples were measured under nitrogen, first heated from 30 °C to 50 °C, then heated at 50 °C increments to 750 °C, with a step size of 0.0145 °C. The powder sample was mixed with ethanol to form a thick slurry, which was dropped onto the platinum stage and allowed to dry. SEM images were acquired on a FEI XL30 Sirion FEG Digital Scanning microscope. Samples were deposited directly on an aluminium stub using double-sided adhesive carbon tape. TEM images were acquired using a FEI Tecnai G2 Sphera microscope. Samples for TEM were prepared by dispersion in ethanol for 10 min in an ultrasonic bath. A drop of the sample was deposited on a lacey-carbon-coated copper grid and allowed to dry before imaging. Magnetization measurements were carried out using a Quantum Design MPMS 5XL superconducting quantum interference device (SQUID) magnetometer. Electrical property measurements were carried out using a Quantum Design Physical Properties Measurement System (PPMS). Four-probe resistivity measurements were carried out on pressed pellets of the samples. To press pellets, a mass of 2×10^3 kg was applied over a bar-shaped pellet of area 1.35 cm $\times$ 0.7 cm. Electrical contacts were established using silver epoxy. Resistivity measurements were also carried out using SiO_2 on Si wafers on which four gold contacts were deposited.

Results and discussion

Monoclinic, metastable VO_2(B) phase

The solvothermal treatment of V_2O_5 suspensions in 30% formaldehyde or isopropanol for 2 days at 180 °C afforded blue-black powders which X-ray analysis confirmed to be the metastable, monoclinic VO_2(B). The patterns were fitted by Rietveld profile analysis (see Fig. 2) and samples from both preparations could be fitted to the monoclinic structure of VO_2(B) (space group $C12/m1$) at 300 K reported by Oka *et al.*[9] The resulting R_w values for the formaldehyde and isopropanol preparations are 6.1% and 6.9%, respectively. No other crystalline phase was observed in either sample. The average particle size, as calculated from Scherrer broadening from the (110) peaks, is 36 nm and 47 nm for the formaldehyde and isopropanol samples respectively.

SEM images of the VO_2(B) sample prepared by formaldehyde reduction of V_2O_5 reveal nanorods with an average width and thickness of 100 nm and 22 nm respectively [see Fig. 3(a)]. The typical nanorod length is found to be 1 μm. The average nanorod width from TEM is 75 nm, with an average thickness in the range of 25 nm. We observe regular interatomic spacing of 0.6 nm

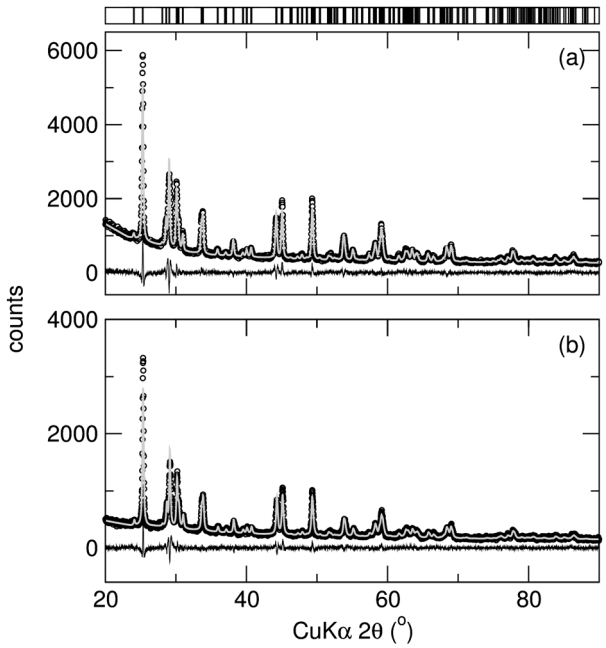

Fig. 2 Observed (○) and calculated (grey line) XRD patterns of monoclinic, metastable VO_2(B), prepared by (a) formaldehyde and (b) isopropanol reduction of V_2O_5. The bottom trace is the difference pattern. The profiles were fitted to the VO_2(B) phase, in space group $C12/m1$. Rietveld analysis gave $a = 12.061$ Å, $b = 3.691$ Å and $c = 6.419$ Å for the formaldehyde sample and $a = 12.068$ Å, $b = 3.696$ Å and $c = 6.418$ Å for the isopropanol sample.

corresponding to the (001) lattice planes for both VO_2(B) samples, similar to those seen by Chen *et al.*[15] Lower-aspect-ratio nanorods (calculated from the average length over the width) were obtained when isopropanol was employed as the reducing agent [see Fig. 3(c), (d)]. The typical nanorod length is 650 nm and the samples prepared in isopropanol were thicker and wider than their counterparts prepared in formaldehyde. Further characterization was performed on the VO_2(B) sample prepared in formaldehyde.

In situ thermodiffractometry experiments were carried out under a nitrogen environment on the VO_2(B) nanorod sample prepared in formaldehyde in order to monitor the transition to the more stable rutile VO_2 phase [see Fig. 4(a)]. The sample was heated from 30 to 50 °C, followed by heating at 50 °C increments to 750 °C. At 30 °C, the observed pattern may be fitted, by Rietveld refinement, to the monoclinic, metastable VO_2(B) structure (space group $C12/m1$) and this remains the predominant phase up to 500 °C. Above this temperature the more stable rutile VO_2 pattern begins to emerge and this becomes the major phase at higher temperatures, up to 750 °C. Rietveld profile analysis of the pattern of the sample after cooling to RT, fitted to the rutile VO_2 phase in space group $P12_1/c1$, with a R_w value of 7.2%. Rietveld analysis was performed on all patterns and the resulting scale factors were extracted for the monoclinic and rutile phases. As seen in Fig. 4(b), up to 400 °C there is no evidence from Rietveld refinement for the presence of rutile VO_2. At 450 °C, the rutile phase begins to appear and reaches a maximum at 550 °C. The emergence of rutile VO_2 is coupled with a decrease of the monoclinic, metastable VO_2(B) phase.

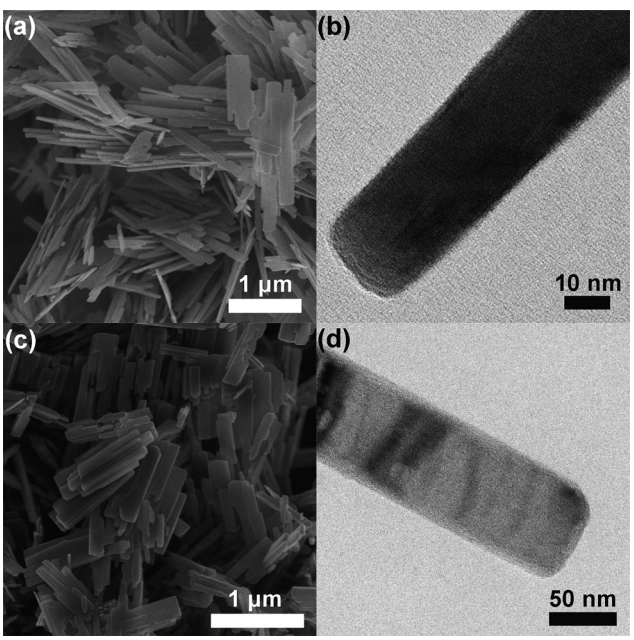

Fig. 3 (a) SEM and (b) TEM images of formaldehyde-reduced metastable VO_2(B) nanorods. The typical nanorod length is 1 μm while the average width and thickness from TEM is 75 nm and 25 nm respectively. A side-on view of one nanorod is shown in (b). (c) SEM and (d) TEM images of isopropanol-reduced metastable VO_2(B) nanorods.

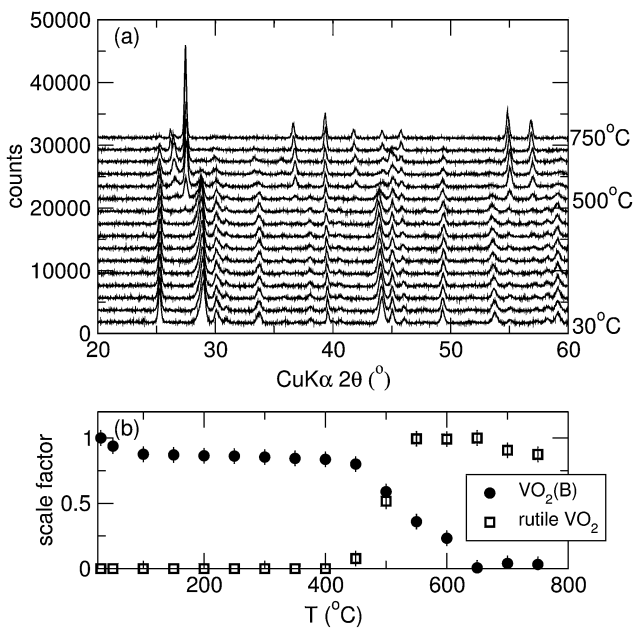

Fig. 4 (a) Thermodiffractometry experiments on the metastable VO_2(B) sample on heating from 30 °C to 50 °C and continuing at 50 °C increments to 750 °C. Note the emergence of the rutile phase at 450 °C, which becomes the sole phase at 750 °C. (b) Emergence of the rutile phase and decrease of the monoclinic phase, monitored using scale factors extracted from Rietveld profile analysis of each pattern recorded.

A further thermodiffractometry experiment was carried out at smaller temperature increments around room temperature. Rietveld analysis of each pattern provided us with a scale factor for the metastable VO_2(B) phase. Interestingly, we noted a decrease in the monoclinic, metastable VO_2(B) scale factor for patterns collected near room temperature at 5 K increments between 300 K and 423 K. A plot of these results is shown in Fig. 5(a). In a previous study by Oka *et al.*, low-temperature X-ray studies performed at 50 K on VO_2(B), revealed a change in the structure compared to a pattern taken at 300 K. These changes were attributed to the transformation from one monoclinic phase at low temperatures to another at high temperatures. Upon the transition from the high-temperature phase to the low-temperature phase, a contraction of the *c*-axis accompanied by an expansion of the *a*- and *b*-axes was noted, caused by a pairing of the V^{4+}–V^{4+} bonds in the low-temperature phase. However, no change in space group is observed. Our study of the Rietveld scale factors recorded for each pattern shows a decrease of the metastable VO_2(B) phase on heating from 300 K to 423 K. We attribute this decrease to a transformation from the low-temperature monoclinic phase to a high-temperature monoclinic phase. Oka and coworkers have also monitored this high-to-low-temperature monoclinic structural change using magnetic measurements.[9]

Our studies of the magnetic behaviour of this material on heating from 100 K to 400 K are shown in Fig. 5(b). We find that the magnetic susceptibility increases on cooling from 400 K to 300 K. Further cooling below 300 K leads to a decrease in the susceptibility, where a dip is noted at 200 K. This decrease is a result of the dimerization of the V^{4+}–V^{4+} ions, leading to the formation of nonmagnetic V–V pairs.[9] This behaviour is in contrast to that of crystalline rutile VO_2, where there is a much sharper decrease in the magnetic susceptibility below its transition temperature.[5]

To date, electrical transport studies have been limited to the work of Liu *et al.*,[13] who noted the semiconducting behavior of VO_2(B) up to 280 K but did not measure across the phase transition. We carried out electrical property measurements on samples of VO_2(B) prepared by the reduction of V_2O_5 in formaldehyde. We found that a first-order transition occurs, similar to that observed for rutile VO_2. In the case of a pressed pellet of material (which has not been sintered), the heating and cooling curves diverge at 290 K. A many-thousand-fold increase in resistivity of this material is observed at 290 K, upon cooling the pellet from 400 K to 150 K. Since the pellet was not sintered, these resistivity values are likely to be higher than those for the individual grains. In order to limit this effect, we also carried out resistance measurements on a wafer onto which four gold contacts were deposited with separations of 3 μm. The sample was prepared by dispersion in ethanol using ultrasound and a drop was deposited and dried on the wafer, where the four contacts meet [see inset of Fig. 6(b)]. In the case of the wafer-deposited nanorods, the maximum resistance value is lower than that observed for the pressed pellet. The cross-sectional area has not been included in the wafer results, since this is a measurement taken on a dried drop of particle suspension and not a pellet. The separation between measurement data acquired on heating and

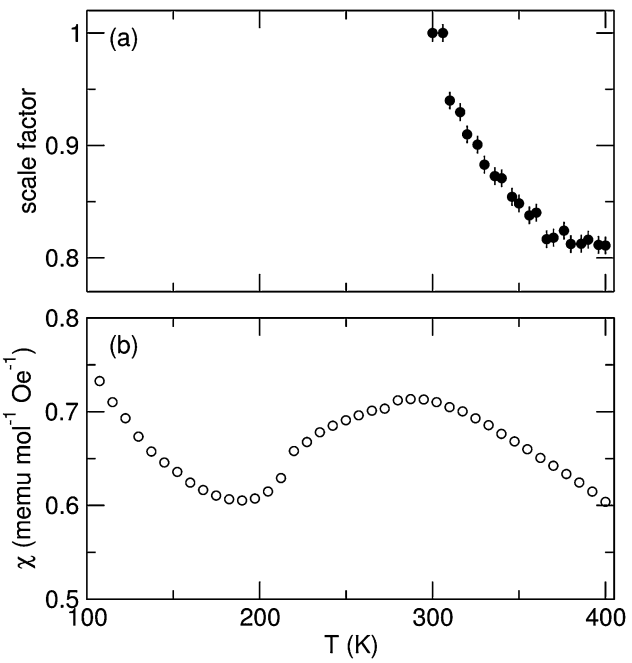

Fig. 5 (a) Rietveld analysis of XRD patterns of the VO_2(B) nanorods prepared by formaldehyde reduction of V_2O_5, collected between 300 K and 423 K, show a decrease in the scale factor of the VO_2(B) phase, likely due to the structural transition to another monoclinic system. (b) Magnetic susceptibility measurement, under a 10 000 Oe field, of monoclinic VO_2(B), prepared by formaldehyde reduction of V_2O_5, on heating from 100 K to 400 K. The field-cooled curve shows a peak centered at approximately 300 K.

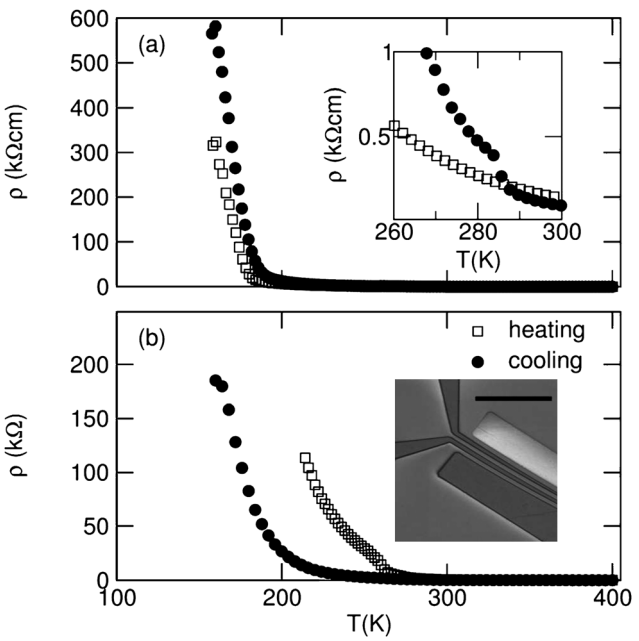

Fig. 6 Resistivity measurements of VO_2(B), prepared by the formaldehyde reduction of V_2O_5, in the form of (a) a pressed pellet and (b) a drop of suspension dried on a wafer fitted with four contacts. A divergence in the heating and cooling curves is noted at ~290 K, where a 10^5-fold increase in resistance is noted on cooling to 150 K. Inset in (a) shows the divergence of the heating and cooling curves which occurs at 290 K. Inset in (b) shows an SEM image of the wafer used. The scale bar measures 50 μm.

cooling is even larger. The change in resistance noted at 290 K is not dissimilar to that found in the case of rutile VO_2, where a 10^5 increase in resistivity is noted at the metal-to-insulator transition temperature at 340 K. It is interesting to note the change in hysteresis behaviour depending on how the sample is prepared. In the case of a pressed pellet, a small hysteresis is observed, while for the sample dispersed and dried on a wafer, a large hysteresis is noted. The first-order nature of the metal–insulator transition requires that nucleation events occur, *i.e.*, the individual nanorods begin to undergo their metal–insulator transitions. When these nanorods are pressed into a pellet, the neighboring nucleation sites set off a chain of transitions since the nanorods are in close proximity. Because the nanorods are present as a pressed pellet of material, there is better nucleation and, hence, a smaller hysteresis is noted. In the case of the wafer, where a suspension of the nanorods has been dried, the nanorods are more spread out and the nucleation events are isolated. The temperature range over which all the samples undergo a metal–insulator transition is larger, noted by the much wider hysteresis curve [see Fig. 6(b)].

Conversion to rutile VO_2 and corundum V_2O_3

Conversion of the VO_2(B) phase to the potentially useful rutile VO_2 phase was achieved by heating the sample at 700 °C for 1 h under argon. The X-ray pattern of the black powder obtained was analyzed by Rietveld refinement [see Fig. 7(a)].

The profile was fitted using the rutile VO_2 phase (space group $P12_1/c1$), with a resulting R_w value of 6.4%. Resistivity measurements of a pressed pellet of material show an insulator-to-metal transition at 340 K, as expected for rutile VO_2 (data not shown). Corundum V_2O_3 was obtained by reducing VO_2(B) in $5\%H_2:95\%N_2$ at 600 °C for 3 h. The X-ray pattern obtained for this sample is shown in Fig. 7(b). The pattern was analyzed by Rietveld refinement and could be fitted to the corundum V_2O_3 phase (space group, $R3CH$), with a resulting R_w value of 7.7%. Scherrer analysis gave an average particle size of 71.5 nm. A metal–insulator transition is found to occur at 140 K, consistent with previous reports (data not shown).[10]

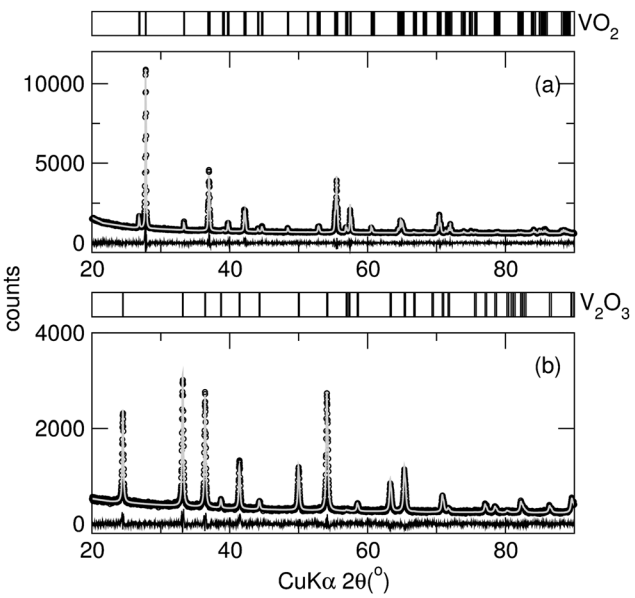

Fig. 7 (a) Observed (○) and calculated (grey line) XRD patterns of rutile VO_2, prepared by heating the formaldehyde-reduced VO_2(B) sample in argon at 700 °C for 1 h. The pattern was fitted using the rutile VO_2 phase. Rietveld analysis gave $a = 5.494$ Å, $b = 4.5237$ Å and $c = 5.380$ Å. (b) Observed (○) and calculated (grey line) XRD pattern of corundum V_2O_3, prepared by reduction in 5% H_2 of the VO_2(B) sample. The pattern was fitted using the corundum V_2O_3 phase. Rietveld analysis gave $a = 4.956$ Å, $b = 4.956$ Å and $c = 14.011$ Å. The bottom trace in both panels is the difference profile.

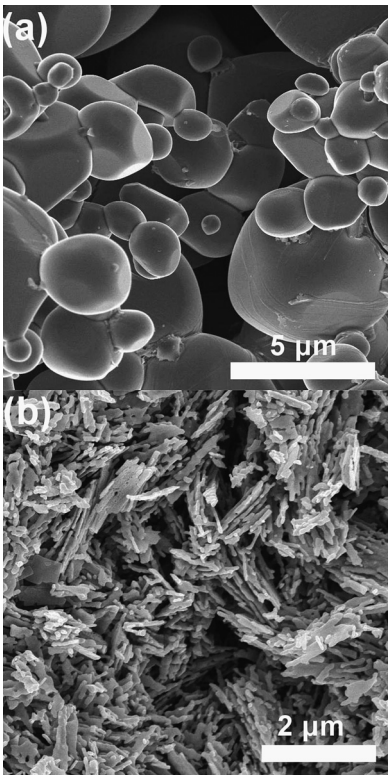

Fig. 8 SEM images of (a) rutile VO_2, prepared by heating the metastable formaldehyde-reduced VO_2(B) sample and (b) corundum V_2O_3 prepared by reduction of the VO_2(B) sample in $5\%H_2:95\%N_2$ at 600 °C for 3 h.

Electron microscopy studies have shown that heating in argon has a pronounced effect on the morphology, with large crystallites of rutile VO_2 obtained (see Fig. 8). The sample size is not monodisperse, with 5 μm crystals observed alongside smaller (1 μm) particles. Electron microscopy images of the corundum V_2O_3 sample reveal that heating in an H_2 environment retains a wire-like morphology, but the appearance of grain-like material indicates that these structures may break up at higher temperatures.

Conclusions

We have prepared metastable VO_2(B) nanorods using either formaldehyde or isopropanol as reducing agents for V_2O_5 by solvothermal methods. We have studied the electrical properties of this metastable VO_2(B) material across the structure transition, where we observe a hysteretic first-order metal–insulator transition around 290 K, associated with the previously reported change in structure. We have found the hysteresis behaviour

differs depending on whether the sample is measured as a pressed pellet or as a dried suspension, owing to a greater degree of neighboring nucleation events in the pressed sample. A 10^5 increase in resistivity is noted upon cooling through the transition temperature. The electrical property measurements on VO_2(B) reported here present a potentially important finding. Rutile VO_2 has been a candidate for a number of important applications owing to the fact that it undergoes an insulator-to-metal transition above 340 K. We have shown that the VO_2(B) phase also goes through a similar transition, albeit at lower temperatures (~290 K). These results open up the possibility of VO_2(B) finding applications in electronics. Magnetic susceptibility measurements and XRD studies confirm a transition occurs at this temperature. This metastable phase may be converted to rutile VO_2 or corundum V_2O_3 depending on the synthetic method employed: heating in argon at 700 °C for 1 h yields nanocrystalline rutile VO_2, while reducing in $5\%H_2 : 95\%N_2$ at 600 °C for 3 h gives corundum V_2O_3.

Acknowledgements

This work was supported by funding from Air Products & Chemicals, Inc. Further support from the UC Discovery program, and from the National Science Foundation (Career Award No. DMR 0449354) and the use of MRSEC facilities (through No. DMR 0520415) is gratefully acknowledged. We thank Brent C. Melot for help with the electrical transport measurements and Jonathan Yuen for providing us with the lithographically-patterned contacts.

References

1 J. Galy and G. Miehe, *Solid State Sci.*, 1999, **1**, 433.
2 F. J. Morin, *Phys. Rev. Lett.*, 1959, **3**, 34.
3 J. B. Goodenough, *J. Solid State Chem.*, 1971, **3**, 490.
4 C. N. R. Rao, *Annu. Rev. Phys. Chem.*, 1989, **40**, 291.
5 A. Zylbersztejn and N. F. Mott, *Phys. Rev. B*, 1975, **11**, 4383.
6 M. M. Qazilbash, M. Brehm, B.-G. Chae, P.-C. Ho, G. O. Andreev, B.-J. Kim, S. J. Yun, A. V. Balatsky, M. B. Maple, F. Keilmann, H.-T. Kim and D. N. Basov, *Science*, 2007, **318**, 1750.
7 P. Baum, D.-S. Yang and A. H. Zewail, *Science*, 2007, **318**, 788.
8 F. Théobald, R. Cabala and J. Bernard, *J. Solid State Chem.*, 1976, **17**, 431.
9 Y. Oka, T. Yao, N. Yamamoto, Y. Ueda and A. Hayashi, *J. Solid State Chem.*, 1993, **105**, 271.
10 S. A. Corr, M. Grossman, J. D. Furman, B. C. Melot, A. K. Cheetham, K. R. Heier and R. Seshadri, *Chem. Mater.*, 2008, **20**, 6396.
11 S. Pavasupree, Y. Suzuki, A. Kitiyanan, S. Pivsa-Art and S. Yoshikawa, *J. Solid State Chem.*, 2005, **178**, 2152.
12 G. Li, K. Chao, H. Peng, K. Chen and Z. Zhang, *Inorg. Chem.*, 2007, **46**, 5787.
13 J. Liu, Q. Li, T. Wang, D. Yu and Y. Li, *Angew. Chem., Int. Ed.*, 2004, **43**, 5048.
14 K. C. Kam and A. K. Cheetham, *Mater. Res. Bull.*, 2006, **41**, 1015.
15 B. S. Guiton, Q. Gu, A. L. Prieto, M. S. Gudiksen and H. Park, *J. Am. Chem. Soc.*, 2005, **127**, 498.
16 X. Chen, X. Wang, Z. Wang, J. Wan, J. Liu and Y. Qian, *Nanotechnology*, 2004, **15**, 1685.
17 G. Armstrong, J. Canales, A. R. Armstrong and P. G. Bruce, *J. Power Sources*, 2008, **178**, 723.
18 F. Sediri and N. Gharbi, *J. Phys. Chem. Solids*, 2007, **68**, 1821.
19 W. Chen, J. Peng, L. Mai, H. Yu and Y. Qi, *Chem. Lett.*, 2004, **33**, 1366.
20 F. Zhou, X. Zhao, H. Xu and C. Yuan, *Chem. Lett.*, 2006, **35**, 1280.
21 C. Leroux, G. Nihoul and G. van Tendeloo, *Phys. Rev. B*, 1998, **57**, 5111.
22 J.-F. Bérar and G. Baldinozzi, *J. Appl. Crystallogr.*, 1993, **26**, 128.